POLITECNICO
MILANO 1863

SCUOLA DI INGEGNERIA INDUSTRIALE
E DELL'INFORMAZIONE

Executive Summary of the Thesis

Experimental and numerical analysis of hybrid CFRP/aluminum laminates response under high-velocity impacts

Laurea Magistrale in Aeronautical Engineering - Ingegneria Aeronautica

Author: Francisco Javier Sanchez Olivera

Advisor: Prof. Paolo Astori

Co-advisor: Ivan Colamartino, Luca Scampini

Academic year: 2022-2023

1. Introduction

In the last decades, the use of composite materials has increased in various structural applications. Especially in the aerospace industry, composites have a preferred role over conventional materials due to their high specific strength, high stiffness, and good fatigue resistance. The rising need of improving the properties of these materials resulted in the creation of a hybrid material made up of thin metal sheets and fiber-reinforced adhesives. FML are composed by alternatively stacking metal and fiber-reinforced composite layers, producing a material that benefits from the characteristics of both materials[1].
Even though the initial goal of creating FML was to improve the fatigue behavior of composites there are several other advantages compared to their constituents. Even though the initial goal of creating FML was to improve the fatigue behavior of composites there are several other advantages compared to their constituents. For example, one of the main advantages of the FML is the high energy absorption due to fiber breakage and shear failure in metallic plates, and high impact resistance[2].

The impact response is of particular interest in the aerospace industry, impact damage of aircraft is caused by various sources. The goal of this work is to find the minimum thickness of carbon, aluminum, and carbon aluminum laminates to stop a projectile at a high speed and develop a numerical model of a carbon/aluminum laminate using the commercial software LS-Dyna and data found from experimental testing[3].

2. Experimental

2.1. Material

2017-T4 aluminum plates were used to produce the impact components. The impact components have the shape 120X120 mm and two different thicknesses 0.5 and 2.5mmm The carbon fiber-reinforced plastic material used for this thesis consists of HexTow® AS4 carbon and HexPly® M79 formulated epoxy resin. The carbon specimens as well as the FML components were produced using the vacuum-assisted bag molding procedure. To enhance the adhesion of the carbon, the FML aluminum layers underwent a surface treatment through sandblasting.

The FML and carbon specimens have the same in-plane dimensions of 120X120 with varying thicknesses, the layout and respective thicknesses are reported in Tables 1 and 2.

2.2. High-Velocity Impact

The high-velocity testing apparatus comprises a gas gun, test specimen support, tested specimens, lights to ensure sufficient illumination for the high-speed camera, and the high-speed camera itself, as depicted in Figure 1.

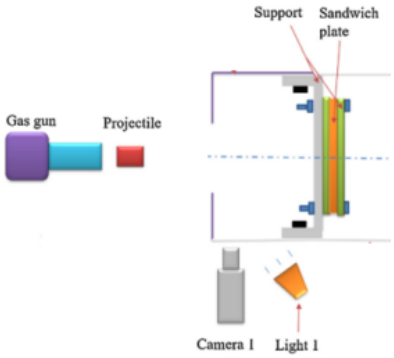

Figure 1: High-Velocity Testing Diagram

Formula 1 is used to determine the constant energy level at which the panels are struck, taking into account both the mass of the 24-gram steel ball projectiles and their velocity of 120 m s^{-1}. To assess the impact resistance of various laminates, this study employs specific energy-absorption parameters that account for both the weight and thickness of the panels.

$$KE = \frac{1}{2} * mv^2 \tag{1}$$

$$SEAM = \frac{KE}{m} \tag{2}$$

$$SEAT = \frac{KE}{t} \tag{3}$$

$$AbsE = KE_{impact} - KE_{residual} \tag{4}$$

These parameters are defined in Formulas 2 and 3. The m in Formula 2 stands for the mass of the laminate, A area of the impacted surface, and the t in Formula 3.6 stands for the thickness of the laminate. Formula 4 shows the formula to compute the absorbed energy of each panel, making reference to the impact and the residual kinetic energy of the projectile.

2.3. Aluminum Impact Response

The process of determining the minimum thickness required to stop the bullet begins by testing progressively thicker materials, starting from the thinnest available. Eventually, a thickness of 2.5 mm is found to effectively stop the projectile. In Table 3, the test results are presented in columns as follows: test id, specimen thickness, impact speed of the projectile, output speed, energy absorbed by the laminate, and residual energy of the bullet.
Thin plates exhibit a more ductile failure mode, allowing the material to absorb more energy by deforming a larger surface area. Conversely, thicker specimens experience a more sudden and shear failure, resulting in less energy absorption and localized deformations.

2.4. Carbon Impact Response

During the initial testing, the first set of specimens exhibited energy absorption below the desired threshold velocity. This was primarily attributed to brittle failure mechanisms observed in the composite materials. However, following the completion of the testing campaign, it was determined that a threshold thickness of approximately 6.8 mm was necessary to achieve the targeted energy absorption at the threshold velocity. The main failure modes include local delamination, fiber breakage, and matrix cracking. These failure mechanisms are significant contributors to energy absorption, as they occur only in a small fraction of the surface area. The results of the impact tests on carbon are summarized in Table 4.

2.5. FML Impact Response

The shooting process of the carbon-aluminum specimens was conducted in two separate campaigns. The first campaign involved the first configuration with 2 aluminum plates, while the second campaign aimed to determine the threshold thickness for a stiffer laminate consisting of 3 aluminum plates. In the first campaign, the threshold thickness for the first configuration was found to be approximately 6.47 millimeters. For the three aluminum plate configurations, the threshold thickness considered was around 5.68 millimeters, as the residual energy was exceptionally low, indicating close to complete energy absorption with less than 2% remaining energy.

ID	Thick [mm]	AL layers	0°-90° plies	±45° plies	Layup
1IFML	2.7	2	4	4	$[\text{AL-0-45-0-45}]_s$
2IFML	5	2	9	9	$[\text{AL-45-0-45-0-45-0-45-0-45}]_s$
3IFML	6.5	2	12	12	$[\text{AL-0-45-0-45-0-45-0-45-0-45-0-45}]_s$
4IFML	3.5	3	4	4	$[\text{AL-0-45-0-45-0.5 AL}]_s$
5IFML	5	3	8	8	$[\text{AL-0-45-0-45-0-45-0-45-0.5 AL}]_s$
6IFML	8.5	3	16	16	$[\text{AL-}[0\text{-}45\text{-}0\text{-}45\text{-}0\text{-}45\text{-}0\text{-}45]_s$ -AL-$[0\text{-}45\text{-}0\text{-}45\text{-}0\text{-}45\text{-}0\text{-}45]_s$-AL]

Table 1: Layup of Impact Carbon Composites

ID	Thick [mm]	AL layers	0°-90° plies	±45° plies	Layup
1IFML	2.7	2	4	4	$[\text{AL-0-45-0-45}]_s$
2IFML	5	2	9	9	$[\text{AL-45-0-45-0-45-0-45-0-45}]_s$
3IFML	6.5	2	12	12	$[\text{AL-0-45-0-45-0-45-0-45-0-45-0-45}]_s$
4IFML	3.5	3	4	4	$[\text{AL-0-45-0-45-0.5 AL}]_s$
5IFML	5	3	8	8	$[\text{AL-0-45-0-45-0-45-0-45-0.5 AL}]_s$
6IFML	8.5	3	16	16	$[\text{AL-}[0\text{-}45\text{-}0\text{-}45\text{-}0\text{-}45\text{-}0\text{-}45]_s$ -AL-$[0\text{-}45\text{-}0\text{-}45\text{-}0\text{-}45\text{-}0\text{-}45]_s$-AL]

Table 2: Layup of Impact Carbon Composites

Test ID	Thick [mm]	Mass [gr]	In V [ms^{-1}]	Out V [ms^{-1}]	Abs E [J]	Res E [J]
1IA	0.5	20	50	0	27.5	Rebound
2IA	0.5	20	101	68	61.34	50.8
3IA	0.5	20	118	100	40.5	110
4IA	2.5	100	103	0	116.7	Rebound
5IA	2.5	100	122	3	163.6	0.1
6IA	2.5	100	144	13	226.4	1.69
7IA	2.5	100	165	96	198.105	101.37

Table 3: Results from Aluminum Impact Tests

Test ID	Thick [mm]	In V [ms^{-1}]	Out V [ms^{-1}]	Abs E [J]	Res E [J]
1IC	2.59	118	89	66	87
2IC	4.7	125	86	90.5	81.35
3IC	5.25	110	58	96	37
4IC	6.8	130	37	170.8	15
5IC	8.8	145	0	231.27	Rebound
6IC	9.61	114	0	142.95	Rebound

Table 4: Results from Impact Tests on Carbon Laminates

A summary of the testing campaign results can be found in Table 5. The material constituents exhibit a combination of ductile and brittle behavior, resulting in a mixed failure mode.

The ductility of aluminum plays a significant role, leading to a larger failure surface by integrating the observed failure modes in the composites.

Test ID	Configuration	T [mm]	In V [ms^{-1}]	Out V [ms^{-1}]	Abs E [J]	Res E [J]
1IFML	AL-C-AL	3.15	118	82	79.2	73.9
2IFML	AL-C-AL	5.55	117	40	135	17.6
3IFML	AL-C-AL	6.44	127	0	177.4	Stuck
4IFML	AL-C-AL-C-AL	3.47	111	68	84.7	50.9
5IFML	AL-C-AL-C-AL	5.68	123	22	161.4	5.32
6IFML	AL-C-AL-C-AL	8	115	0	1477	Rebound

Table 5: Results from Impact Tests on FML

The carbon-aluminum specimens exhibit identifiable failure modes, including ductile dents, crack propagation, shear failure of aluminum, detachment at the carbon-aluminum interface, delamination, matrix cracking, and fiber breakage from the carbon constituent.
Interestingly, the three aluminum configurations demonstrate the ability to absorb more energy and distribute it effectively across the contact area. This enhanced energy absorption can be attributed to the higher ductility provided by the additional aluminum foil in these configurations.

3. Numerical Analysis

The numerical model consists of a bullet and a plate made of shell elements. Initially, the bullet is represented as a solid sphere mesh with a diameter of 18 mm. The mesh has a density of 5, meaning there are 5 elements along the radius. Different material models are tested to examine significant plasticity effects in steel projectiles. A plastic model is initially used, but it is determined that the plastic strain is negligible. As a result, an elastic material is chosen instead.
The plate used in the impact test is modeled with a 4-node mesh, selected to match dimensions of 120 x 120 mm. It's worth noting that a 20 x 20 mm section of the plate is fixed as a clamp using a set of nodes restricting the displacement and rotations in all directions to replicate the test conditions in the rig.
The bullet is positioned at 5 mm of distance from the plate, this is made in order to save computational time on the projectile's travel distance. The simulation time is fixed to 0.001 seconds and 2.5e-5 time intervals for the D3 plot to have a good understanding of the interaction between the late and the bullet.

3.1. Aluminum Model

In order to account for the anticipated failure modes and energy absorption characteristics of aluminum, an elastoplastic constitutive law must be used to approximate its behavior. The LS-DYNA material type 24 (*MAT 024) is the prevailing material model for simulating impact events involving elastoplastic, isotropic materials[4].
Two main parameters can be adjusted to refine the model: the mesh and the strain to failure. Initial results indicated that a highly refined mesh resulted in a flexible and weak plate. To address this, a coarser mesh was employed for both aluminum thicknesses, making the plate stiffer. This modification enabled the plate to absorb more energy compared to the initial iteration. The second parameter to be modified is the strain to failure. By raising the plastic strain to failure to 0.19 compared to the original 0.18, a stronger plate was obtained.
To evaluate the model's accuracy against experimental results, the total energy of each component is computed. The residual energy of the projectile is determined by analyzing the remaining energy after impact, while the absorbed energy by the plate indicates its ability to absorb energy. A comparison between the deformed shapes can be seen in Figure 2 and Table 6 shows the experimental and simulated results.

3.2. Carbon Model

LS-DYNA presents a vast choice in terms of orthotropic material models. References in suggest the use of material type 58 to model a composite plate. The experimental plates surpass the numerical model in terms of strength when it comes to carbon. To address this issue, the solution involves adjusting the mesh density and manipulating the strain-to-failure values [6].

Test ID	Mass[gr]	In V [ms^{-1}]	Abs E [J]	Test ID	Abs E [J]	Error [%]
1SA	20	50	28.4	1IA	27.5	Rebound
2SA	20	101	51	2IA	61.3	16.5
3SA	20	118	21	3IA	40.5	48
4SA	100	116	120	4IA	116	Rebound
5SA	100	122	169	5IA	163	Rebound
6SA	100	144	144	6IA	226	36.39
7SA	100	165	113	7IA	198	43

Table 6: Comparison between experimental and numerical aluminum analysis

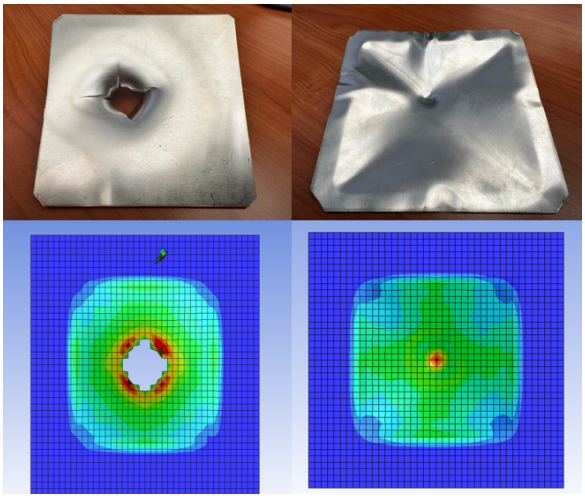

Figure 2: Left: Thick specimen. Right: Thin specimen.

Unlike the single strain-to-failure used in aluminum, there are now five different strains considered: tensile longitudinal, compressive longitudinal, tensile transversal, compressive transversal, and shear strain. To enhance the plate's strength, the mesh from the aluminum case was reused, while the strains were scaled to minimize the material's alteration. A scaling factor of 1.5 was chosen as a compromise between thin and thick specimens.
Due to the brittle nature of the material and its lack of ductility, the plate exhibits no plastic deformation. Consequently, the failure is sudden and localized primarily in the center of the plate, which differs from the behavior observed in the aluminum case. A comparison between deformed shapes is reported in Figure 3 and Table 7 shows the comparison between experimental and numerical impacts.

3.3. FML Model

The interaction between composite laminate and the metal plates is modeled as an adhesive interface that is mainly dominated by the delamination phenomena. This adhesion interface modeling has several approaches in LS-DYNA, the two main approaches used in FML are tiebreak contacts and adhesive elements [5].
Tiebreak contacts are widely used and considered a reliable and relatively simple contact algorithm. To simulate the adhesive interface of a CFRP-AL laminate and model the delamination behavior between its constituents, the CONTACT_AUTOMATIC_ONE_WAY_SURFACE _TO_SURFACE _TIEBREAK contact card is employed. One-way contact types allow for compression loads to be transferred between the slave nodes and the master segments.
In order to evaluate and develop numerical models for FML laminates, a differentiation was made between the two tested configurations. Firstly, the weaker configuration consisting of two aluminum plates is discussed. The model is constructed based on existing models of aluminum and carbon that have already undergone refinement through adjustments in mesh and strain to failure. For the FML model, only the PARAM parameter governing the distance at which the bonding between aluminum and carbon is disrupted got manipulated. The numerical model of the FML exhibited significantly lower strength compared to the experimental counterpart. To enhance the strength of the laminate, the PARAM parameter was increased to 0.85.

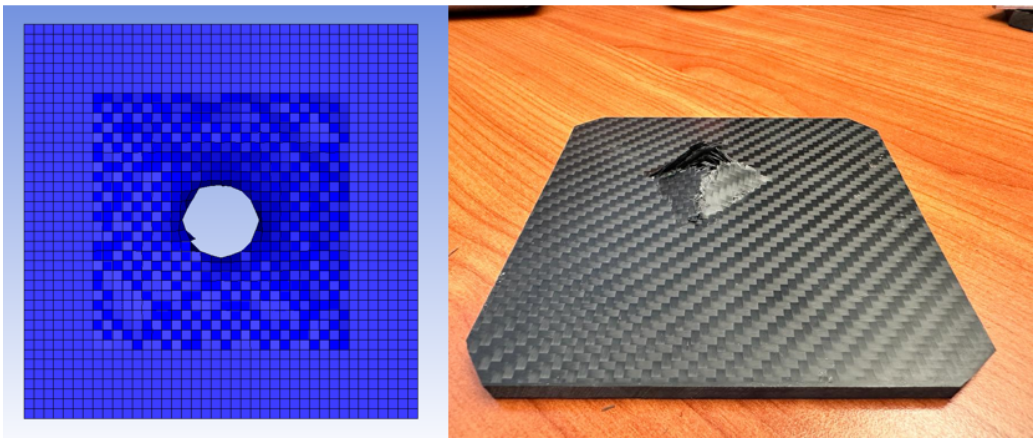

Figure 3: Left: Simulated carbon specimen. Right: Experimental carbon specimen.

Test ID	Mass[gr]	In V [ms^{-1}]	Abs E [J]	Test ID	Abs E [J]	Error [%]
1SC	55	118	51	1IC	66	22.7
2SC	100	125	90.8	2IC	90.5	0.3
3SC	110	110	103.8	3IC	96.1	8
4SC	150	130	142	4IC	170	16.8
5SC	195	145	190.8	5IC	231	Rebound
6SC	200	115	148	6IC	143	Rebound

Table 7: Comparison between experimental and numerical carbon analysis

In comparison to the two aluminum plates, the numerical model of the three aluminum plates appears excessively rigid. Despite utilizing the appropriate materials and PARAM parameters based on previous simulations, even the thinner components remain without being penetrated. Interestingly, the additional layer of aluminum located in the center of the laminate demonstrates a higher capacity for absorbing energy and resists penetration. Table 8 presents a comparison between the experimental and numerical results of FML components, Figure 4 shows the deformed experimental and numerical shapes.

4. Material Comparisons

Since the amount of energy is similar for all the threshold thicknesses a more useful comparison can be made while comparing the absorbed energy capabilities normalized with respect to changing properties of the laminates. The comparison can be seen from two perspectives, the amount of energy absorbed per mass unit and a second approach considering the amount of energy per unit of thickness.

Table 9 presents the results of the experimental campaign for the different laminates.
In Figure 5, the graph illustrates the specific energy absorption per unit mass for various materials. A clear observation from the graph is that aluminum is the most effective material for energy absorption in lightweight structures. It required nearly half the mass compared to the two-aluminum configuration FML to halt the bullet across different speeds. The other materials displayed similar behavior, as they required an equivalent mass to stop the bullet. This indicates that while the FML outperforms carbon in energy absorption, the additional weight contributed by aluminum makes the two solutions comparable in terms of overall weight.
Figure 6 illustrates the specific energy absorption per unit thickness for different laminates. The advantage of aluminum over other materials in terms of space efficiency is clearly apparent. Aluminum requires less than half the thickness compared to other materials to stop the bullet. This indicates that in applications where thinness is crucial, aluminum outperforms the rest.

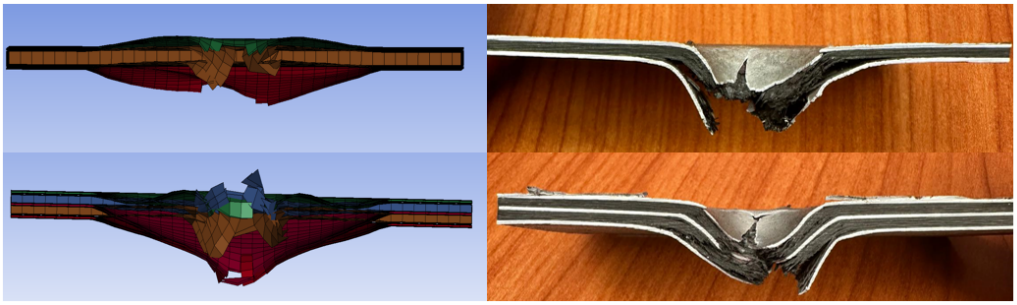

Figure 4: Top: Numerical and experimental comparison of impacted two aluminum configuration. Bottom: Numerical and experimental comparison of impacted three aluminum configuration.

Test ID	Mass[gr]	In V [ms^{-1}]	Abs E [J]	Test ID	Abs E [J]	Error [%]
1SFML	80	118	67.3	1IFML	79.2	15
2SFML	135	118	100.9	2IFML	135.5	25.5
3SFML	160	127	183	3IFML	177	Rebound
4SFML	100	111	140	4IFML	84.6	Rebound
5SFML	140	123	172	5IFML	161	Rebound
6SFML	190	115	155	6IFML	145	Rebound

Table 8: Comparison between experimental and numerical FML analysis

Test ID	In V [ms^{-1}]	T [mm]	Mass [gr]	Abs E [J]	Res E [J]	SEAM	SEAT
5IA	122	2.5	100	163.6	0.1	1636	65.44
4IC	130	6.8	150	170.8	15	1138.7	19.4
3FML	127	6.5	160	177.4	0	1108.8	27.3
5FML	123	5.48	140	161	5.3	1150	29.4

Table 9: Results from threshold thicknesses of the different materials

Another observation is that as the number of aluminum plies in the fiber metal laminate increases, the component can be made even thinner. It is possible that an FML with four aluminum plates could potentially be the thinnest solution after pure aluminum. Carbon, on the other hand, ranks last in terms of slim solutions, suggesting that composites are not the most favorable option for impact energy absorption applications. Although implementing FML may enhance absorption characteristics, aluminum remains the most optimal solution.

5. Conclusions

The primary focus was to determine the most optimal solution for stopping a steel sphere projectile at speeds around 120 m/s through experimental testing. The results demonstrated that aluminum was the superior choice, considering both weight and space-saving considerations. Additionally, the experiments clearly showed that while the FML exhibited better energy absorption compared to the pure carbon specimen, the inclusion of aluminum increased the weight and negated any weight advantages. However, the introduction of aluminum did enhance the material's ductility, potentially resulting in a thinner solution.

These findings indicate that carbon is the least efficient method for energy absorption upon impact. Despite its ability to absorb a significant amount of energy through localized failure, the brittle failure of carbon proves to be less effective compared to the ductile failure observed in aluminum. Although an FML with more aluminum layers could potentially offer a more lightweight and space-saving solution compared to the carbon and previously presented FML configura-

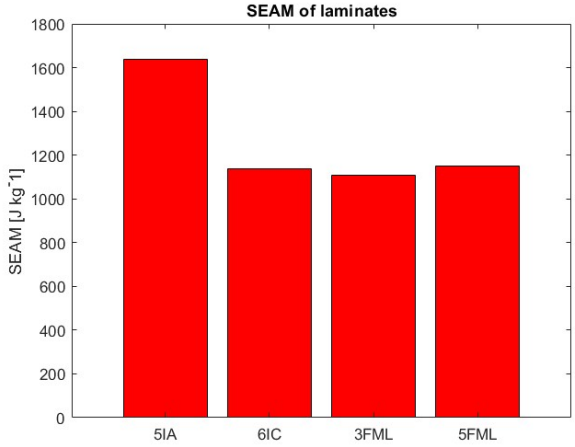

Figure 5: Specific energy absorption per unit mass of each material.

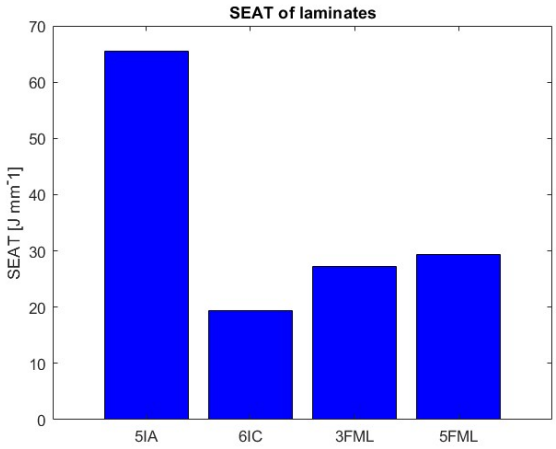

Figure 6: Specific energy absorption per unit thickness of each material.

tions, it cannot compete with pure aluminum.

The second primary objective of this study was to develop numerical models using LS Dyna for the impact materials. A successful numerical model was provided up to the threshold. To enhance the modeling of the materials under investigation, further refinements can be implemented. This includes developing a more sophisticated model using defined user cards in LS-Dyna, which enables greater control and customization of the simulation parameters. Additionally, incorporating cohesive elements into the model would provide a more accurate representation of the adhesive interface between the constituents of the FML. Cohesive elements are known to offer a precise solution for modeling such interfaces.

To evaluate the performance of solid elements, a simulation campaign utilizing aluminum material was conducted. Surprisingly, the results obtained from the simulation aligned significantly better with the experimental results. This finding highlights the potential for developing a more precise model to accurately replicate the impact response. The results are shown in Table 10. The composite laminates were initially observed to be composed of thick shell elements, which was not an efficient application of shell elements. To address this issue, an alternative solution was implemented by creating sub-laminates of 1 mm thickness, resulting in more efficient and thinner shell elements. The outcomes of this approach are presented in Table 6.3, demonstrating that the sub-laminate solution yields a weaker but more accurate representation of the behavior of thick laminates compared to the original single laminate solution.

Test ID	T [mm]	In V [ms^{-1}]	Abs E_{sim}[J]	Abs E_{exp}[J]	$Error_{shell}$[%]	$Error_{solid}$[%]
1SFML	2.7	118	120	79.2	51	15
2SFML	5	117	154.79	135	14	23
3SFML	6.5	127	177.4	177.4	Stuck	Rebound
4SFML	3.5	111	135.5	84.7	Rebound	Rebound
5SFML	5	123	161.4	161.4	Rebound	Rebound
6SFML	8.5	115	147.5	147	Rebound	Rebound

Table 10: Comparison between experimental and numerical FML analysis

Test ID	T [mm]	In V [ms^{-1}]	Abs E_{sim}[J]	Abs E_{exp}[J]	$Error_{shell}$[%]	$Error_{sub}$[%]
1SC	2.5	118	44	66	22.7	33.3
2SC	4	125	79.4	90.5	0.3	12
3SC	5.3	110	93.2	96	8	3
4SC	7.2	130	149.3	170.8	16.8	12
5SC	8.8	145	173.2	231.27	Rebound	Rebound
6SC	10.5	114	142.2	142.2	Rebound	Rebound

Table 11: Comparison between experimental and numerical carbon analysis

References

[1] J.W. Gunnink A. Vlot. Fiber metal laminates – an introduction. *Kluwer Academic Publisher*, 2001.

[2] Benedictus R. Alderliesten RC. Fiber/metal composite technology for future primary aircraft structures. *Structures, Structural Dynamics and Materials Conference*, 2007.

[3] M. Sadighi Alderliesten RC, Benedictus R. Impact resistance of fiber-metal laminates: A review. *International Journal of Impact Engineering*, 2012.

[4] N. E. Dowling. Mechanical behavior of materials: Engineering methods for deformation, fracture and fatigue, third edition. *Choice Reviews Online*, 2007.

[5] J. Hallquist. Ls dyna theory manual. 2006.

[6] LSTC. Ls dyna keyword user's manual iii. 2015.